View metadata, citation and similar papers at core.ac.uk

brought to you by CORE

provided by Elsevier - Publisher Connector

Vailable online at www.sciencedirect.com

SciVerse ScienceDirect

Energy Procedia 27 (2012) 253 – 258

Energy Procedia

SiliconPV 2012, 03-05 April 2012, Leuven, Belgium

Statistical Evaluation of a Luminescence-based Method for imaging the series resistance of solar cells

H. Höffler, J. Haunschild, R.Zeidler, S. Rein

Fraunhofer Institut for Solar Energy Systems ISE, Heidenhofstr. 2, 79110 Freiburg, Germany
Tel.: +49(0)761/4588-5651, E-mail: hannes.hoeffler@ise.fraunhofer.de

Abstract

In the last years photoluminescence (PL) imaging has become a standard characterization method for conventional silicon solar cells and wafers providing spatially resolved information for material characterization and process control. In this work, the method of the **c**oupled determination of **d**ark saturation **c**urrent and series **r**esistance (C-DCR) is evaluated on conventional silicon solar cells in terms of its accuracy, reliability and informative value based on a large number of conventional multicrystalline silicon solar cells. The statistical evaluation is based on a comparison of the series resistance mean values obtained from the C-DCR method with the global values obtained from the IV-characteristics within the standard cell testing. Furthermore, examples for its application are given and demonstrate that the minimum exposure time needed for the C-DCR method is short enough to allow an inline application of the method.

© 2012 Published by Elsevier Ltd. Selection and peer-review under responsibility of the scientific committee of the SiliconPV 2012 conference. Open access under CC BY-NC-ND license.

Keywords: luminescence; characterization; solar cells

1. Introduction

In the last years different methods have been developed to extract spatially resolved information about series resistance and dark saturation current quantitatively from electroluminescence (EL) and photoluminescence (PL) images [1-6]. For none of these methods, reliability has been investigated on a statistically relevant number of solar cells. As the method of **c**oupled determination of **d**ark saturation **c**urrent and series **r**esistance (C-DCR) is used as a standard characterization technique at Fraunhofer ISE since 2009, statistical data from production are evaluated here to demonstrate the reliability and benefit of this quality control technique which is used offline so far. In the present study the discussion focusses on series resistance images only, while the results for dark saturation current images will be published

1876-6102 © 2012 Published by Elsevier Ltd. Selection and peer-review under responsibility of the scientific committee of the SiliconPV 2012 conference. Open access under CC BY-NC-ND license.
doi:10.1016/j.egypro.2012.07.060

elsewhere. First, the analytical approach of the C-DCR technique is summarized and an example for application is given. Second, the results from almost three years application are evaluated. Finally, the inline applicability of the method is discussed.

2. Principle of the C-DCR method

The C-DCR method was first presented in Ref. [6]. It combines the techniques of EL and PL. Hence the application of an external voltage to the solar cell and the illumination of the solar cell. The method is based on the assumption that the luminescence intensity of one pixel in an image $I(x,y)$ is given by:

$$I(x,y) = C(x,y)e^{\frac{V(x,y)}{V_T}} + B(x,y)\, j_{sc} \quad (1)$$

Here $C(x,y)$ and $B(x,y)$ are constants which need to be determined, $V(x,y)$ is the local voltage at the pn-junction, V_T is the thermal voltage at 25°C and j_{sc} is the short circuit current density at the given illumination conditions. Initially, two images $I_{low-voc}(x.y)$ and $I_{low-jsc}(x.y)$ are taken at low illumination under open circuit and short circuit conditions, respectively. From these two images using $I_{low-jsc}(x,y) = B(x,y) * j_{sc}$ the calibration constant $C(x,y)$ is determined by:

$$C(x,y) = \frac{I_{low-voc}(x,y) - I_{low-jsc}(x,y)}{e^{(V_{cal-voc}/V_T)}} \quad (2)$$

The important assumption made here is that $V(x,y)$ from equation (1) has no spatial dependence at low illumination conditions and can be substituted by $V_{cal-voc}$ which is the measured global voltage of the image $I_{low-voc}(x,y)$. For low illumination conditions, an illumination intensity of 0.2 suns is used. To determine the series resistance topography, three more images are required: (i) $I_{high-jsc}(x,y)$ at high illumination (1 sun) and short circuit conditions and (ii) $I_{high-1st}(x,y)$ and $I_{high-2nd}(x,y)$ at high illumination (1 sun) and two different applied voltages. Using equation (1) yields:

$$V_{1st}(x,y) = V_T * \ln\left(\frac{I_{high-1st}(x,y) - I_{high-jsc}(x,y)}{C(x,y)}\right) \quad (3)$$

with $V_{1st}(x,y)$ being the local voltage at the pn-junction of the $I_{high-1st}(x,y)$ image. The same equation can be derived for $I_{high-2nd}(x,y)$. So, two different images are obtained which are calibrated to the local voltage at the pn-junction under the applied operating conditions [4].

To evaluate the voltage calibrated images with respect to recombination losses and series resistance losses, the C-DCR method makes use of the terminal connected diode model. Each pixel in the image is considered as a diode whose local current-voltage characteristics are approximated by a one-diode model with the dark saturation current $j_0(x,y)$ and which is connected via a local series resistance $R_S(x,y)$ to the external contacts, where the external voltage V_{appl} is applied and measured. This model yields [7]:

$$R_S(x,y) = \frac{V_{appl} - V(x,y)}{j_0(x,y) * e^{(V(x,y)/V_T)} - j_{sc}} \quad (4)$$

For the two voltage-calibrated images $I_{high,1st}(x,y)$ and $I_{high,2nd}(x,y)$ taken under two different operating conditions, Equation (4) yields a system of two equations which can be solved analytically to determine the two unknown variables $R_S(x,y)$ and $j_0(x,y)$ for each pixel of the image..

3. Examples of application

The C-DCR method allows a separation of series resistance losses arising e.g. from metallization defects and recombination losses arising e.g. from material defects, which cause a high dark saturation current density. Fig. 1 exemplary shows images of an industrial mc-Si solar cell.

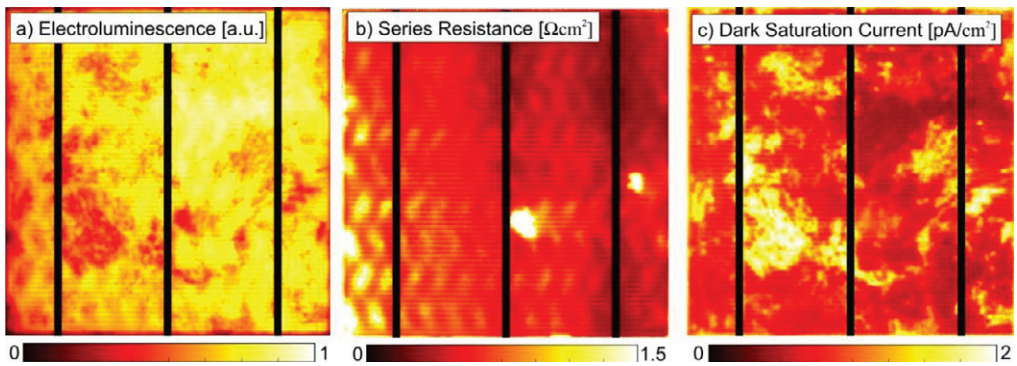

Fig. 1. (Left) EL-image of a conventional mc-Si solar cell. (Middle) R_s image of the example cell. (Right) j_0 image of the example cell. While recombination and series resistance losses appear superposed in the EL image, both loss mechanisms and the related defects are separated in the R_s and the j_0 image

The example cell shows metallization problems and areas of high recombination due to material defects. In the EL image (Fig. 1a) both features induced by both defect classes are superposed and can therefore hardly be separated. On the contrary, in the extracted R_s image (Fig. 1b) two defect signatures become clearly visible. The two bright spots near the bus bars originate from interrupted contact fingers at the front side metallization grid. The pattern which gets brighter towards the left edge of the image can be attributed to a poor formation of the metal semiconductor contact at the rear side which is induced by a locally wrong firing temperature. In the extracted j_0 image on the other hand (Fig. 1c), bright areas can be clearly attributed to areas of increased recombination at dislocation sites.

4. Statistical evaluation of the C-DCR method

At the end of each solar cell process the dark and illuminated IV-characteristics of the cells are routinely measured in an inline IV-tester. To get local information, the C-DCR method is used as standard characterization technique at Fraunhofer ISE since 2009. Typically 5-20 % of the solar cells are selected from each solar cell batch and measured at the offline luminescence imaging tool with a resolution of 160 µm/pixel. For the statistical analysis presented here, a total number of 565 solar cells coming from 35 solar cell batches have been evaluated by means of C-DCR. The solar cell batches cover a wide variety of solar cell concepts (Al-BSF cells, LFC-PERC cells), wafer geometries (156x156cm^2, 125x125cm^2) and material types (mc-Si, Cz-Si) as well as a variety of processes which leads to wide range of R_s values from 0.39–14.6 Ωcm^2. From the IV-characteristics a global value of R_s is calculated using the method by Aberle et al. [8], which is based on a comparison of the dark and the illuminated IV-characteristic at the maximum power point. The R_s values based on the C-DCR measurements were calculated as the arithmetic mean [9] of local $R_s(x,y)$ values in the R_s image.

Fig. 2 (left) shows the comparison of the global R_s-values from IV-testing and C-DCR. Fig. 2 (middle) shows enlarged the section marked in Fig. 2 (left). Fig. 2 (right) shows the relative deviation $dev_{rel}(R_s)$ of the two R_s measurement methods.

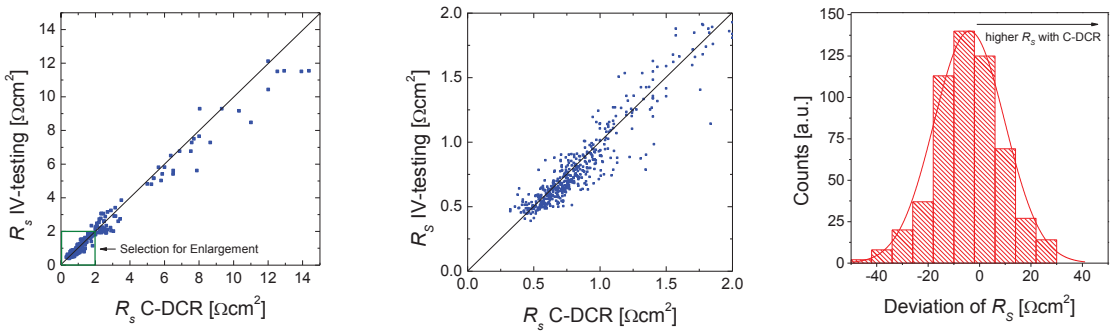

Fig. 2. (Left) Comparison of the global R_s values gained from C-DCR and standard *IV*- testing. The dataset contains 565 solar cells with a broad variety. The deviation from the bisecting line is small. (Middle) Enlargement of the R_s comparison for small R_s values which are most relevant in terms of production. (Right) Histogram of the relative deviation of the two R_s values. The R_s values from C-DCR are on average about 4% lower than the values from standard *IV*-testing

The correlation of the two methods is good both for small and high R_s values. The deviation for solar cells with very high R_s values can be explained by severe local problems which cause inaccuracies in both methods. The scattering for typical R_s values between 0.5–1.0 Ωcm^2 can partly be explained by tool specific differences of the contacting units of the IV and the luminescence tool.

As can be seen from the deviation histogram in Fig. 2 (right), the averaged R_s values from C-DCR are approx. 4% lower than the global R_s values extracted from the IV-characteristics. The lower R_s values from C-DCR may originate from differences of the contacting units in both techniques. In the C-DCR measurement the Aluminum rear side of the solar cell is contacted flat-like, while in the IV-measurement only the soldering pads on the rear side are contacted by a series of point-contacts. Hence, the current paths for charge carriers leaving the solar cell at the rear are different in both setups: while there is only a vertical current flow in the case of the C-DCR measurement due to the flat back contact, there is an additional horizontal current flow in the rear side metallization towards the point contacts in the case of the IV measurement, which increases the R_s losses.

Evaluating the accuracy of luminescence-based R_s methods, it has to be kept in mind that these methods focus more on detecting local R_s inhomogeneities than on providing accurate R_s values, as these local information are highly valuable for trouble shooting and process optimization. Nevertheless, the good correlation of the global R_s values from C-DCR and IV-testing, found here in a statistics from almost three years application at Fraunhofer ISE, strongly increases the quantitative reliability of the results obtained from the C-DCR technique.

5. Inline applicability of the C-DCR method

The five PL images which are needed for the C-DCR method to calculate R_s and j_0 topographies as shown in Fig. 1 are usually taken with a total camera exposure time of 26 s. To test the inline applicability of the C-DCR method, the five pictures have been recorded with different exposure times, the total measurement time ranging from 26 s down to 0.13 s.

Fig. 3 (left) shows for three different solar cells the mean R_s values from C-DCR images taken with different acquisition times. The three samples cover a broad R_s range: sample 1 exhibits strong R_s losses due to a non-ideal emitter sheet resistance and a related high contact resistance, sample 2 shows medium R_s values due to non-ideal process conditions during fast firing and sample 3 shows low R_s values as they are typical defect-free solar cells. As can be seen from Fig. 3 (left), the mean R_s values from the C-DCR images are only slightly affected by the acquisition time and only increase slightly for very small total

measurement times well below 1 s. The reason for this behavior can be observed in Fig. 3 (right) which shows the histograms of the C-DCR R_s images from sample 3 for the different total exposure times. For rather high total exposure times above 10 s, the signal-to-noise level and the mean R_s values more or less remain the same. If total exposure time is further reduced, noise starts to affect the results and leads to a broadening of the histogram and thus to an increase of the mean R_s value.

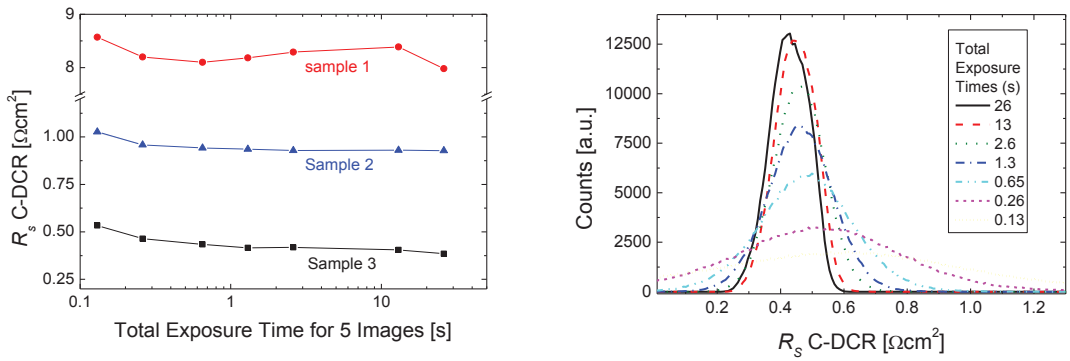

Fig. 3. (Left) The mean R_s value from C-DCR images as a function of the total measurement time for three different samples. Due to noise the values increase slightly for short acquisition times. (Right) Histograms of the R_s images of sample 3 for different total exposure times. The noise increases with decreasing total exposure time, shifts the mean R_s value to higher values and reduces the spatial information in the images (see Fig. 4)

From the smoothing of the histograms, the conclusion may be drawn that the images lose their informative value in terms of the localization of R_s defects for small total exposure times. In Fig. 4 the R_s image of sample 2 is shown which exhibits the typical conveyer belt pattern indicating contact formation problems. The marked section is enlarged on the right and shown for different total exposure times.

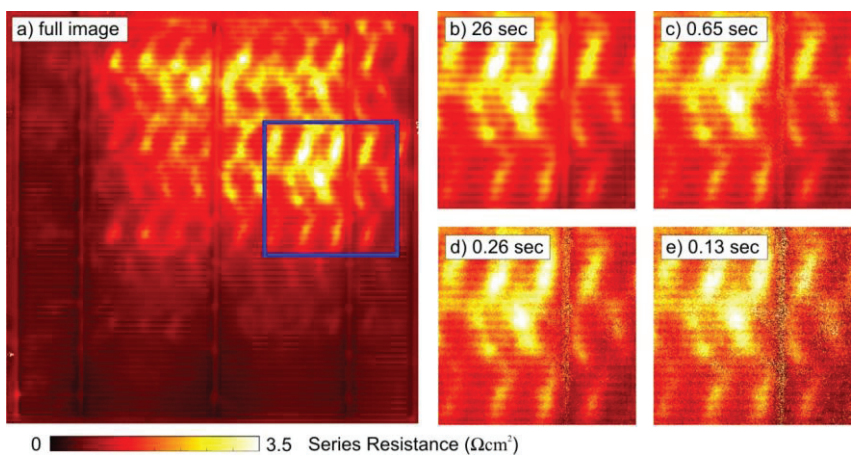

Fig. 4. (a) Full R_s image measured by means of the C-DCR technique on sample 2. (b-e) Enlarged section marked in (a) for different total exposure times, displayed in the images. Although noise increases, the relevant pattern is still clearly visible in the image with lowest total exposure time

Although noise significantly influences especially the images with shortest acquisition times, the relevant features can still be clearly observed. To be inline applicable, the total data acquisition time has to be below one second to meet production speed. As can be seen from Fig. 3 and 4 this is already

achieved with the present setup. Further improvements of camera sensitivity should allow even lower total exposure times without further decreasing the signal-to-noise ratio. Whether the signal-to-noise ratio of these images is sufficient for an automated reliable detection of relevant image features strongly depends on the applied image processing algorithms, which will be investigated in a next step.

6. Conclusion

In this work, the spatially resolved values for the series resistance obtained from the C-DCR technique are compared to the global R_s values obtained from IV measurements for a dataset of 565 samples taken from 35 solar cell batches within the last three years. A good quantitative correlation of both R_s values is found in the whole range from very high to low R_s values. These results demonstrate that the C-DCR technique not only provides valuable spatial information about R_s defects but also reliable quantitative information which makes the technique even more valuable for the final solar cell inspection. It has been shown that the typical data acquisition time may be reduced well below 1 s without losing the relevant image signatures of the R_s defects in spite of a decreasing signal-to-noise ratio. That is why the C-DCR technique has become a standard method for quality control at Fraunhofer ISE and is ready for inline application.

Acknowledgements

We thank our colleagues at Fraunhofer ISE for fruitful discussions and support in solar cell processing. This work has been supported by the Fraunhofer Society under the frame of the project ABICS-LUM.

References

[1] Breitenstein O, Khanna A, Augarten Y, Bauer J, Wagner J-M and Iwig K. Quantitative evaluation of electroluminescence images of solar cells. *Physica Status Solidi RRL 4* (2010); **1**7-9.

[2] Haunschild J, Glatthaar M, Kasemann M, Rein S and Weber ER. Fast series resistance imaging for silicon solar cells using electroluminescence. *Physica Status Solidi RRL* (2009); **3** (7-8): 227 - 229.

[3] Hinken D, Ramspeck K, Bothe K, Fischer B and Brendel R. Series resistance imaging of solar cells by voltage dependent electroluminescence. *Applied Physics Letters* (2007); **91**182104-1-3.

[4] Trupke T, Pink E, Bardos RA and Abbott MD. Spatially resolved series resistance of silicon solar cells obtained from luminescence imaging. *Applied Physics Letters* (2007); **90**093506-1-3.

[5] Kampwerth H, Trupke T, Weber JW and Augarten Y. Advanced luminescence based effective series resistance imaging of silicon solar cells. *Applied Physics Letters* (2008); **93** (202102): 202102/1-3.

[6] Glatthaar M, Haunschild J, Kasemann M, Giesecke J, Warta W and Rein S. Spatially resolved determination of dark saturation current and series resistance of silicon solar cells. *Physica Status Solidi RRL* (2010); **4** (1): 13-15.

[7] Glatthaar M, Haunschild J, Zeidler R, Demant M, Greulich J, Michl B et al. Evaluating luminescence based voltage images of silicon solar cells. *Journal of Applied Physics* (2010); **108**014501.

[8] Aberle AG, Wenham SR and Green MA. *A new method for accurate measurements of the lumped series resistance of solar cells*. Proceedings of the 23rd IEEE PVSC. Louisville, Kentucky, USA, 1993. pp. 133-9.

[9] Michl B, Kasemann M, Giesecke J, Glatthaar M, Schütt A, Carstensen J et al. *Application of luminescence imaging based series resistance measurement methods in an industrial environment*. Proceedings of the 23rd EU-PVSEC. Valencia, Spain, 2008. pp. 1176-81.